ELSEVIER Thermochimica Acta 249 (1995) 199–210

thermochimica
acta

Preparation, characterisation and thermal behaviour of *N*-(3-aminopropyl)-1,3-propanediamine complexes of nickel(II) in the solid state

Chandi Pariya, Ashutosh Ghosh [1], Nirmalendu Ray Chaudhuri *

Department of Inorganic Chemistry, Indian Association for the Cultivation of Science,
Calcutta-700 032, India

Received 8 April 1994; accepted in final form 9 June 1994

Abstract

The complexes $[Ni(dpt)_2]X_2 \cdot nH_2O$ (where dpt is *N*-(3-aminopropyl)-1,3-propanediamine; $n = 0$ when X is I, NCS or ClO_4; $n = 1$ when X is Cl, Br or NO_3; $n \gg 1$ when X is $0.5SO_4$ and $0.5SeO_4$), $Ni(dpt)X_2 \cdot nH_2O$ ($n = 0$ when X is Cl or NO_3; $n = 1$ when X is Br or I; $n = 2$ when X is NO_3; $n = 3$ when X is $0.5SO_4$ or $0.5SeO_4$), $[Ni(aepn)_2)]I_2$, $Ni(aepn)I_2$ (where aepn is *N*-(2-aminoethyl)-1,3-propanediamine), $[Ni(dien)_2]I_2$ and Ni(-dien)I_2 (where dien is diethylenetriamine) have been synthesised from the solution and thermal investigations upon them have been carried out in the solid state. $[Ni(dpt)_2]X_2$ (X is Br or NO_3) undergoes endothermic reversible phase transitions upon heating (198–212°C, $\Delta H = 3.5$ kJ mol^{-1} and 205–222°C for $[Ni(dpt)_2]Br_2$ and $[Ni(dpt)_2](NO_3)_2$ respectively). $Ni(dpt)I_2$ shows exothermic irreversible phase transition during heating (193–220°C; $\Delta H = 4.1$ kJ mol^{-1}). The thermal stabilities of dpt complexes are compared with those of the corresponding aepn and dien complexes.

Keywords: DTA; Nickel compound; Phase transition; Stability; TG; XRD

---

* Corresponding author.

[1] Present address: Department of Chemistry, Jhargram Raj College, Jhargram-721 507, West Bengal, India.

0040-6031/95/$09.50 © 1995 – Elsevier Science B.V. All rights reserved

SSDI 0040-6031(94)01936-B

1. Introduction

Complexes with saturated five-membered rings are more stable than those with six-membered rings: this fact has been shown in case of the chelated complexes with diethylenetriamine (dien), *N*-(2-aminoethyl)-1,3-propanediamine (aepn) and *N*-(3-aminopropyl)-1,3-propanediamine (dpt) by measurement of stability constants [1] and thermochemical studies [2].

$H_2N{-}CH_2{-}CH_2{-}NH{-}CH_2{-}CH_2{-}NH_2$
(dien)

$H_2N{-}CH_2{-}CH_2{-}NH{-}CH_2{-}CH_2{-}CH_2{-}NH_2$
(aepn)

$NH_2{-}CH_2{-}CH_2{-}CH_2{-}NH{-}CH_2{-}CH_2{-}CH_2{-}NH_2$
(dpt)

However, no comparative data regarding their solid state thermal stabilities were available in the literature. Recently, the results of thermal analysis of dien and aepn complexes of Ni(II) have been published from our laboratory [3–6]. There, in addition to the thermal stabilities we observed several novel phase transformation phenomena, occurring due to either conformational changes of the individual chelate rings or geometrical isomerism. Here we report the thermal investigations of Ni(II) dpt complexes of varying anions along with the Ni(II) iodide complexes of dien and aepn which were not reported earlier and the results obtained are compared with those of dien and aepn complexes [3–6].

2. Experimental

High purity *N*-(3-aminopropyl)-1,3-propanediamine, *N*-(2-aminoethyl)-1,3-propanediamine and diethylenetriamine were purchased from Aldrich Chemical Company Inc. and used as received. All other chemicals were AR grade. The equipment employed to record IR spectra, electronic spectra, X-ray powder diffraction data, elemental analyses and thermal measurements (TG–DTA and DSC) has been described [7]. The far-IR spectra were recorded in FTIR spectrometer (Polytech FIR-30). Elemental analyses, thermal parameters, X-ray powder diffraction data and the comparative chart of initial temperature of decomposition are shown in Tables 1, 2, 3 and 4, respectively.

2.1. Preparation of the complexes

$[Ni(dpt)_2]Cl_2 \cdot H_2O$ (**1**), $Ni(dpt)Cl_2$ (**1c**), $Ni(dpt)(NCS)_2$ (**6a**), $[Ni(dpt)_2](NO_3)_2 \cdot H_2O$ (**7**), $Ni(dpt)(NO_3)_2 \cdot 2H_2O$ (**7c**), $Ni(dpt)(NO_3)_2$(**7d**) and $[Ni(dpt)_2](ClO_4)_2$ (**8**) were prepared following the methods described in the literature [8,9].

$[Ni(dpt)_2]Br_2 \cdot H_2O$ (**2**), $[Ni(dpt)_2]I_2$ (**3**), $[Ni(dpt)_2](NCS)_2$ (**6**), $[Ni(aepn)_2]I_2$ (**9**) and $[Ni(dien)_2]I_2$ (**10**) were prepared by the same methods as those adopted above.

$Ni(dpt)Br_2 \cdot H_2O$ (**2d**), $Ni(dpt)I_2$ (**3a**), $Ni(aepn)I_2$ (**9a**) and $Ni(dien)I_2$ (**10a**) were prepared by adding triamine (1 mmol) dropwise with constant stirring to the corresponding metal salt (1 mmol) in ethanolic medium (10 cm^3). On keeping the resulting solution in a desiccator for several days, fine green crystals separated out. These were filtered, washed with ethanol and stored in a desiccator.

$Ni(dpt)AO_4 \cdot 3H_2O$ (A is S or Se) were prepared according to the same procedure as in the case of (**2d**) but using water instead of ethanol as solvent. $[Ni(dpt)_2]AO_4 \cdot nH_2O$ (A is S or Se; $n \gg 1$) were prepared by adding triamine (2 mmol) slowly to the corresponding metal salt (1 mmol) in water–ethanol (1:3) mixture (15 cm^3). The resulting solution was evaporated to dryness in a rotary evaporator. The species obtained after evaporation was washed thoroughly with dry ethanol and stored in a vacuum desiccator. These complex species are highly hygroscopic.

$[Ni(dpt)_2]Cl_2$ (**1a**), $Ni(dpt)Cl_2$ (**1b**), $[Ni(dpt_2]Br_2$ (**2a**), $Ni(dpt)Br_2$ (**2c**), $Ni(dpt)I_2$ (**3b**), $Ni(dpt)SO_4$ (**4a**), $Ni(dpt)SeO_4$ (**5a**) and $[Ni(dpt)_2](NO_3)_2$ (**7a**) were prepared by the temperature arrest technique in the solid state.

3. Results and discussion

3.1. Characterisation of the complexes

$[Ni(dpt)_2]X_2 \cdot H_2O$ (X is Cl, Br or NO_3) and $[Ni(dpt)_2]X_2$ (X is NO_3 or NCS) possess octahedral geometry and an N_6 chromophore as is evident from their magnetic moments and electronic spectral data (Table 1). The octabhedral bis-dpt complexes can exist in three geometrical isomeric forms, namely s-*fac* (I), u-*fac* (II) and *mer* (III) as shown in Fig. 1. Unlike the dien complexes, however, there is no well established method to characterise the geometrical isomers of dpt complexes using IR spectra. Therefore, we have chosen the complex *mer*-$[Ni(dpt)_2](ClO_4)_2$, whose structure has been analysed by X-ray single crystallography [9] as a model complex. A comparison of the IR spectra of all the bis complexes to those of *mer*-$[Ni(dpt)_2](ClO_4)_2$ reveals that almost all the IR active vibrations of dpt are identical indicating the *mer* geometry. In the case of sulphate and selenate, bis complexes are extremely hygroscopic. As a result physicochemical studies in the solid state could not be done. However by considering the colour of the complexes and the ligational behaviour of dpt together with the thermal decomposition pattern, it is assumed that these two species also possess an N_6 chromophore like the other bis complexes.

All the mono complexes are octahedral as is evident from their magnetic and electronic spectral data (Table 1). Some of the species, e.g. $Ni(dpt)X_2$ (X is Cl or NCS), were reported earlier [8,10], where pseudo-octahedral geometry was proposed. The far-IR spectrum of $Ni(dpt)Cl_2$ shows band at 165, 215 and 254 cm^{-1} for ν(Ni–Cl); the bands appearing at 165 and 215 cm^{-1} are interpreted as ν_b(Ni–Cl) whilst the band at 254 cm^{-1} is interpreted as ν_t(Ni–Cl) [11]. However, in the case of $Ni(dpt)Br_2$ these bands shift to 125 cm^{-1} for ν_b(Ni–Br) and 190 cm^{-1} for ν_t(Ni–Br). There is no structural evidence for mono-dpt complexes of Ni(II), although Cannas et al. [12] have reported the structure of $Cd(dpt)Cl_2$ as dimeric

Table 1

Elemental analysis, magnetic and electronic (mull) spectral data of triamine complexes of nickel(II)

Complex	No.	Colour	Elemental analysis/% [a]			μ_{eff}/ BM	λ_{max}/ nm
			C	H	N		
$[Ni(dpt)_2]Cl_2 \cdot H_2O$	**1**	Blue	35.2 (35.1)	8.7 (8.8)	20.4 (20.5)	3.2	564, 360
$[Ni(dpt)_2]Cl_2$	**1a**	Blue	36.5 (36.7)	8.7 (8.7)	21.3 (21.4)	3.1	606, 372
$Ni(dpt)Cl_2$	**1c**	Green	27.5 (27.6)	6.4 (6.5)	16.0 (16.1)	3.3	651, 388
$[Ni(dpt)_2]Br_2 \cdot H_2O$	**2**	Blue	29.0 (28.9)	7.0 (7.2)	16.7 (16.8)	3.2	560, 356
$[Ni(dpt)_2]Br_2$	**2a**	Blue	29.7 (29.9)	7.2 (7.1)	17.5 (17.5)	3.2	575, 302
$Ni(dpt)Br_2 \cdot H_2O$	**2d**	Green	19.7 (19.6)	5.1 (5.2)	11.3 (11.4)	3.1	646, 314
$Ni(dpt)Br_2$	**2c**	Green	20.4 (20.6)	5.0 (4.9)	12.0 (12.0)	3.2	665, 396
$[Ni(dpt)_2]I_2$	**3**	Blue	25.2 (25.0)	5.8 (5.9)	14.5 (14.6)	3.2	584, 378
$Ni(dpt)I_2 \cdot H_2O$	**3a**	Green	15.4 (15.6)	4.3 (4.1)	9.0 (9.1)	3.1	642, 382
$Ni(dpt)I_2$	**3b**	Green	16.3 (16.2)	3.9 (3.8)	9.5 (9.5)	3.1	671, 395
$Ni(dpt)SO_4 \cdot 3H_2O$	**4c**	Light blue	21.1 (21.2)	6.6 (6.8)	12.3 (12.4)	3.2	606, 370
$Ni(dpt)SeO_4 \cdot 3H_2O$	**5c**	Light blue	18.4 (18.6)	5.8 (5.9)	10.9 (10.9)	3.3	606, 386
$[Ni(dpt)_2](NCS)_2$	**6**	Blue	38.3 (38.4)	7.8 (7.8)	25.6 (25.6)	3.2	570, 353
$Ni(dpt)(NCS)_2$	**6a**	Blue	31.1 (31.4)	5.2 (5.6)	22.6 (22.9)	3.3	567, 391
$[Ni(dpt)_2](NO_3)_2 \cdot H_2O$	**7**	Blue	30.8 (31.1)	7.7 (7.8)	24.1 (24.2)	3.1	559, 354
$[Ni(dpt)_2](NO_3)_2$	**7a**	Blue	32.1 (32.3)	7.5 (7.6)	25.1 (25.2)	3.2	563, 370
$Ni(dpt)(NO_3)_2 \cdot 2H_2O$	**7c**	Blue	20.4 (20.6)	6.1 (6.0)	19.9 (20.0)	3.1	548, 350
$Ni(dpt)(NO_3)_2$	**7d**	Blue	22.6 (22.9)	5.3 (5.4)	22.1 (22.3)	3.2	558, 365
$[Ni(dpt)_2](ClO_4)_2$	**8**	Blue	27.6 (27.7)	6.7 (6.5)	16.1 (16.1)	3.2	566, 353
$[Ni(aepn)_2]I_2$	**9**	Blue	21.6 (21.9)	5.7 (5.5)	15.2 (15.3)	3.1	592, 370
$Ni(aepn)I_2$	**9a**	Green	14.0 (14.0)	3.4 (3.5)	9.8 (9.8)	3.2	608, 381
$[Ni(dien)_2]I_2$	**10**	Blue	23.0 (23.1)	4.8 (5.0)	16.2 (16.2)	3.1	587, 367
$Ni(dien)I_2$	**10a**	Green	11.6 (11.5)	3.3 (3.1)	10.0 (10.1)	3.1	598, 372

[a] Percentages in parentheses are theoretically calculated values. Elemental analysis of $[NiL_2]AO_4 \cdot nH_2O$ (A is S or Se; $n \gg 1$) could not be done due to extreme hydroscopic character, and hence the composition has been drived from their TG curves (Fig. 6).

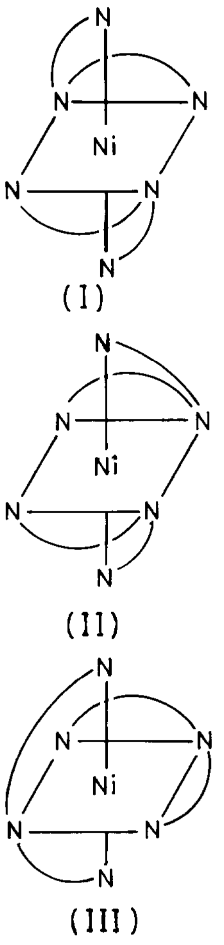

Fig. 1. Schematic drawings of s-*fac* (I), u-*fac* (II) and *mer* (III) isomers of [Ni(dpt)$_2$] ion.

units having C_2 symmetry and a cis configuration. Coordination around cadmium is octahedral with one chlorine atom acting as a bridge and it is interesting to note that the IR spectrum of the complex Ni(dpt)X_2 (X is Cl or Br) is almost the same as that of Cd(dpt)Cl_2. Considering all these facts we propose the structure of Ni(dpt)X_2 (X is Cl or Br) shown in Fig. 2(I). Ni(dpt)X_2 complexes (X is I or NCS) are also expected to be of similar geometry. The IR spectrum (in nujol) of Ni(dpt)$(NO_3)_2$ possesses four bands at 1730, 1752, 1771 and 1782 cm^{-1} for the combination band of the ν_1 symmetric stretching and the doubly degenerate in-plane bending mode of NO_3 ion, indicating the presence of unidentate together with bidentate nitrato groups. Therefore, a monomeric octahedral geometry as reported by Curtis and Curtis [13] is proposed for [Ni(dpt)$(NO_3)_2$]. An aquation-deanation reaction with visual change in colour of Ni(dpt)$(NO_3)_2$ on storage in humid atmosphere was reported [8]. This phenomenon is also observed in Ni(dpt)Cl_2,

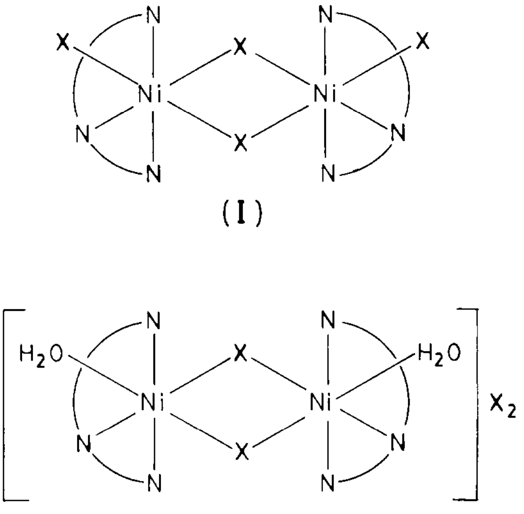

(I)

(II)

Fig. 2. Proposed structure of [Ni(dpt)X_2] where X is Cl or Br (I) and Ni(dpt)$X_2 \cdot H_2O$ (where X is Br I) (II).

whereas Ni(dpt)Br_2, NiLI_2 (L is dien, aepn or dpt) and Ni(dpt)$(NCS)_2$ do not undergo any such transformation. This suggests that in Ni(dpt)Cl_2 halide ion bridging is ruptured in humid atmosphere, whereas this does not take place in the cases of the corresponding bromo, iodo and thiocyanato complexes.

Ni(dpt)$AO_4 \cdot 3H_2O$ complexes (A is S or Se) are light blue in colour. These complexes are monomeric taking three molecules of water within the coordination sphere to attain octahedral geometry, whereas the anhydrous species is light green in colour. Electronic spectral band shifts to a lower energy region occur on dehydration, although the magnetic susceptibility value appears to be the same (Table 1).

It may be noted that Ni(dpt)$(NCS)_2$ crystals are not hydrated even on crystallisation from water. However Ni(dpt)X_2 complexes (X is Br or I) always crystallise as Ni(dpt)$X_2 \cdot H_2O$. These become dehydrated upon heating without any visual colour change and dehydrated on storage in open atmosphere. The probable structure of Ni(dpt)$X_2 \cdot H_2O$ (X is Br or I) is shown in Fig. 2(II), on the basis of an earlier report [14].

3.2. Phase transition of the complexes

Upon heating [Ni$(dpt)_2$]$Br_2 \cdot H_2O$ (**2**) and [Ni$(dpt)_2$]$(NO_3)_2 \cdot H_2O$ (**7**) become anhydrous without any visual colour change at about 130 and about 138°C respectively (see Table 2). The anhydrous species (**2a**) and (**7a**) undergo a reversible phase transition on further heating (198–212°C, $\Delta H = 3.5$ kJ mol^{-1} (Fig. 3) and 205–222°C respectively). The ΔH value for the transformation (**7a** → **7b**) is not

Table 2
Thermal parameters of triamine complexes of nickel(II)

Thermally induced reactions	Temperature range/°C	DTA peak temperature/°C	
		Endo	Exo
$[Ni(dpt)_2]Cl_2 \cdot H_2O$ (**1**) → $[Ni(dpt)_2]Cl_2$ (**1a**)	75–158	142	–
$[Ni(dpt)_2]Cl_2$ (**1a**) → $Ni(dpt)Cl_2$ (**1b**)	197–240	232	–
$Ni(dpt)Cl_2$ (**1b**) → $NiCl_2$	275–400	304	280
$Ni(dpt)Cl_2$ (**1c**) → $NiCl_2$	282–400	309	–
$[Ni(dpt)_2]Br_2 \cdot H_2O$ (**2**) → $[Ni(dpt)_2]Br_2$ (**2a**)	70–130	92	–
$[Ni(dpt)_2]Br_2$ (**2a**) → $[Ni(dpt)_2]Br_2$ (**2b**)	198–212	204	–
$[Ni(dpt)_2]Br_2$ (**2b**) → $Ni(dpt)Br_2$ (**2c**)	230–288	256	–
$Ni(dpt)Br_2$ (**2c**) → $NiBr_2$	288–410	325[a]	–
$Ni(dpt)Br_2 \cdot H_2O$ (**2d**) → $Ni(dpt)Br_2$ (**2c**)	110–140	124	–
$[Ni(dpt)_2]I_2$ (**3**) → NiI_2	238–370	257, 272	–
$Ni(dpt)I_2 \cdot H_2O$ (**3a**) → $Ni(dpt)I_2$ (**3b**)	68–130	80, 104	–
$Ni(dpt)I_2$ (**3b**) → $Ni(dpt)I_2$ (**3c**)	193–220	–	206
$Ni(dpt)I_2$ (**3c**) → NiI_2	227–342	250[a], 265	240
$[Ni(dpt)_2]SO_4 \cdot nH_2O$ (**4**) → $[Ni(dpt)_2]SO_4$ (**4a**)	30–145	82, 110	–
$[Ni(dpt)_2]SO_4$ (**4a**) → $Ni(dpt)SO_4$ (**4b**)	208–234	225	–
$Ni(dpt)SO_4$ (**4b**) → $NiSO_4$	290–355	318	–
$Ni(dpt)SO_4 \cdot 3H_2O$ (**4c**) → $Ni(dpt)SO_4$ (**4b**)	80–120	98	–
$[Ni(dpt)_2]SeO_4 \cdot nH_2O$ (**5**) → $[Ni(dpt)_2]SeO_4$ (**5a**)	30–140	85, 132	–
$[Ni(dpt)_2]SeO_4$ (**5a**) → $Ni(dpt)SeO_4$ (**5b**)	180–250	243	–
$Ni(dpt)SeO_4$ (**5b**) → $NiSeO_4$	270–325	–	312
$Ni(dpt)SeO_4 \cdot 3H_2O$ (**5c**) → $Ni(dpt)SeO_4$ (**5b**)	78–137	120	–
$[Ni(dpt)_2](NCS)_2$ (**6**) → $Ni(NCS)_2$	186–410	158[a], 260	327
$Ni(dpt)(NCS)_2$ (**6a**) → $Ni(NCS)_2$	248–420	272	294, 368
$[Ni(dpt)_2](NO_3)_2 \cdot H_2O$ (**7**) → $[Ni(dpt)_2](NO_3)_2$ (**7a**)	115–138	129	–
$[Ni(dpt)_2](NO_3)_2$ (**7a**) → $[Ni(dpt)_2](NO_3)_2$ (**7b**)	205–222	217	–
$[Ni(dpt)_2](NO_3)_2$ (**7b**) → [b]	225–250	240	–
$Ni(dpt)(NO_3)_2 \cdot 2H_2O$ (**7c**) → $Ni(dpt)(NO_3)_2$(**7d**)	180–215	198	–
$Ni(dpt)(NO_3)_2$(**7d**) → [b]	215–260	227	–
$[Ni(aepn)_2]I_2$ (**9**) → NiI_2	231–352	287, 309	243
$Ni(aepn)I_2$ (**9a**) → NiI_2	250–340	272, 295	261
$[Ni(dien)_2]I_2$ (**10**) → NiI_2	296–358	318, 333	302
$Ni(dien)I_2$ (**10a**) → NiI_2	322–370	358	337

[a] Peak due to melting. [b] Decompositions are complicated.

shown because partial decomposition starts before completion of the transition (Fig. 4). The nature of the reversible phase transitions (**2a** → **2b** and **7a** → **7b**) remains unexplored due to the lack of facilities for obtaining spectral and structural data at higher temperatures. $Ni(dpt)I_2 \cdot H_2O$ (**3a**) becomes anhydrous at about 128°C and transforms to (**3b**) in two overlapping steps as is evident from its TG–DTA curves. On dehydration two anions situated outside the coordination sphere (Fig. 2(I)) become coordinated to nickel(II) in place of the water molecule and the resulting colour change is from green to greenish yellow. This is reflected in the electronic spectral band (642 nm) which shifts to higher wavelength (663 nm) on dehydration. The dehydrated species (**3b**) shows an exothermic irreversible phase

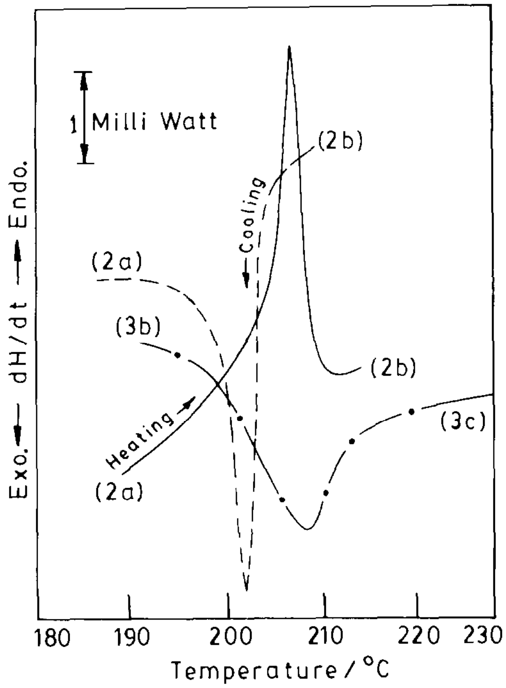

Fig. 3. DSC curves of $[Ni(dpt)_2]Br_2$ (**2a**) (sample mass 8.3 mg), (——) for heating and (– – –) for cooling, and $Ni(dpt)I_2$ (**3b**) (sample mass 5.9 mg) (– · – · –).

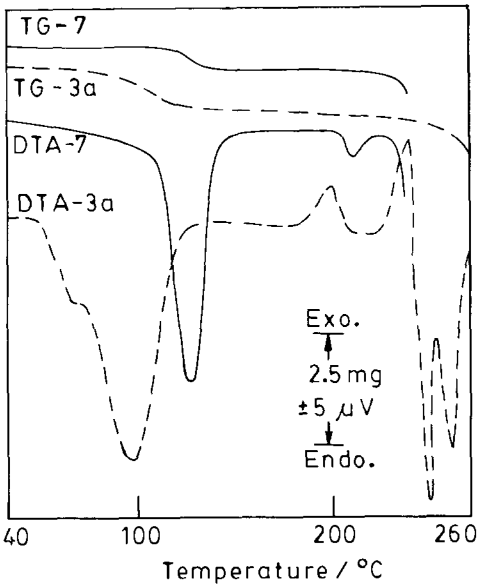

Fig. 4. TG–DTA curves of $[Ni(dpt)_2](NO_3)_2 \cdot H_2O$ (**7**) (sample mass 10.7 mg) (——), and $Ni(dpt)I_2 \cdot H_2O$ (**3a**) (sample mass 11.4 mg) (– – –).

Table 3
Prominent lines d/Å in the X-ray powder diffraction patterns of the complexes

$Ni(dpt)I_2$ (**3b**)		$Ni(dpt)I_2$ (**3c**) [a]	
8.51 vw	3.74 vs	8.59 vw	3.38 vw
8.12 vw	3.61 s	8.51 vw	3.33 w
7.34 vw	3.45 m	8.04 w	3.25 m
6.81 s	3.30 w	7.76 w	3.21 s
5.47 m	3.01 m	7.25 m	3.06 m
5.28 vw	2.95 w	6.71 m	2.95 vw
4.93 m	2.88 w	5.44 w	2.73 w
4.80 vs	2.75 m	4.65 s	2.42 w
4.75 s	2.55 w	4.62 m	2.36 vw
4.40 m	2.37 w	3.87 m	
4.29 m	2.31 vw	3.71 vw	

Key: s, strong; m, medium; w, weak; vs, very strong; vw, very weak.

[a] The species obtained after the phase transition of (**3c**) was cooled in a desiccator and its X-ray powder diffraction patterns were taken immediately.

transformation (193–220°C, $\Delta H = 4.1$ kJ mol^{-1} (Fig. 3)) with no visual colour change. The X-ray powder diffraction pattern of (**3b**) and its after phase species (**3c**) are different (Table 3) indicating a major change in unit cell structure. However, the IR spectra of these two species are quite similar except in the region around 1000 cm^{-1} where $\rho_w(CH_2)$, $\rho(CH_2)$, $\tau(NH_2)$ and $\nu(NH_2)$ vibrational bands appear. Therefore, the phase transition is assumed to be due to a change in crystallinity along with the conformational changes in the chelate rings.

3.3. Decomposition of the complexes

Upon heating $[Ni(dpt)_2]X_2 \cdot H_2O$ complexes (X is Cl, Br or NO_3) undergo dehydration and transform to the corresponding anhydrous complex species. The complex $[Ni(dpt)_2]Cl_2$ (**1a**) starts to decompose at about 197°C and transforms to $NiCl_2$ at about 400°C via $Ni(dpt)Cl_2$ (**1b**) as is evident from the noticeable plateau in the TG curve (Fig. 5). The intermediate species $Ni(dpt)Cl_2$ (**1b**) shows an exothermic peak followed by endothermic peak during decomposition. However $Ni(dpt)Cl_2$ (**1c**) derived from aqueous solution (see Section 2) shows no such exothermic peak. $Ni(dpt)Cl_2$ (**1b**) can be stored in a desiccator but it transforms to $Ni(dpt)Cl_2 \cdot nH_2O$ ($n \gg 1$) on storage in open atmosphere. The hydrated species on reheating becomes $Ni(dpt)Cl_2$ (**1c**). $[Ni(dpt)_2]Br_2$ decomposes similarly to its chloro analogue. As is evident from its TG curve the intermediate species $Ni(dpt)Br_2$ is found to be a mixture. As a result we could not synthesise its mono species by the temperature arrest technique in the solid state. The decomposition of $[Ni(dpt)_2]X_2$ (X is NO_3, I or NCS) is complicated. On heating $[Ni(dpt)_2]AO_4 \cdot nH_2O$ complexes (A is S or Se; $n \gg 1$) become dehydrated at about 125 and about 140°C for the sulphate and selenate complexes respectively. Then on further heating they transform to the corresponding metal salts via the thermally stable mono-triamine

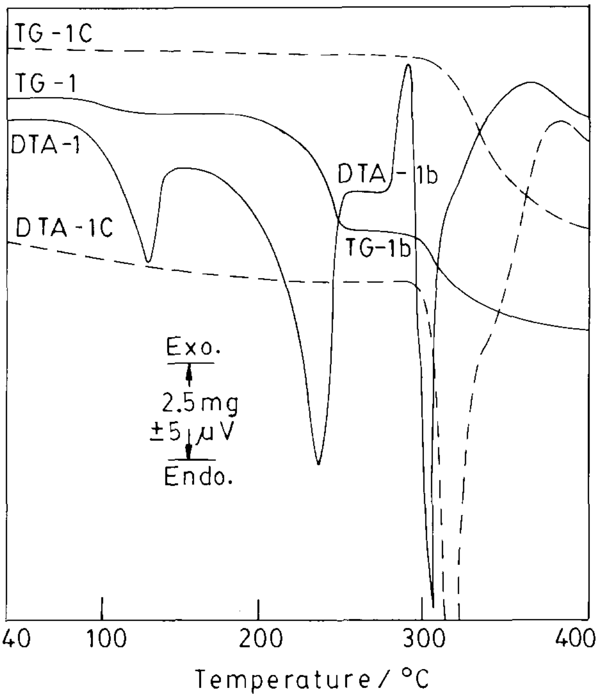

Fig. 5. TG–DTA curves of $[Ni(dpt)_2]Cl_2 \cdot H_2O$ (**1**) (sample mass 14.2 mg) (——) and $Ni(dpt)Cl_2$ (**1c**) (sample mass 12.4 mg) (– – –).

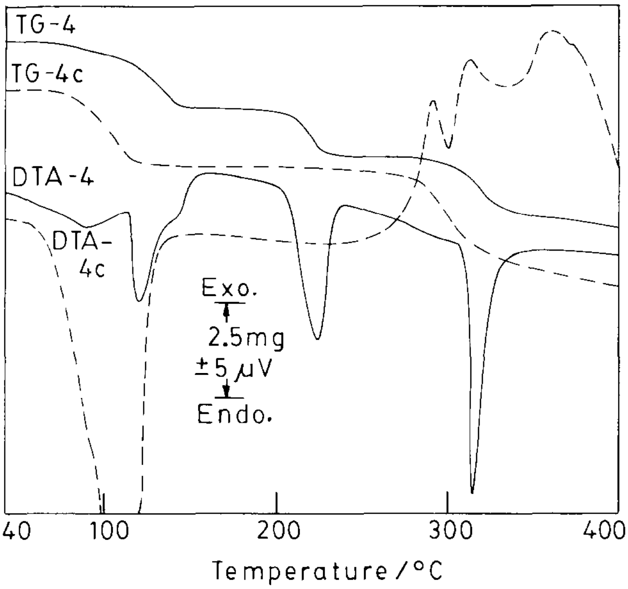

Fig. 6. TG–DTA curves of $[Ni(dpt)_2]SO_4 \cdot nH_2O$ (**4**) (sample mass 13.2 mg) (——), and $Ni(dpt)SO_4 \cdot 3H_2O$ (**4c**) (sample mass 11.5 mg) (– – –).

Table 4
Comparative chart of T_i (initial temperature of decomposition in °C) for some of the bis- and mono-triamine of nickel(II)

Complex	L		
	dien	aepn	dpt
$[NiL_2]Cl_2$	284	270	197
$NiLCl$	285	274	270
$[NiL_2]Br_2$	302	270	230
$NiLBr_2$	332	293	280
$[NiL_2]I_2$	296	231	227
$NiLI_2$	322	250	230
$[NiL_2]SO_4$	290	262	208
$NiLSO_4$	331	320	260
$[NiL_2]SeO_4$	260	209	180
$NiLSeO_4$	290	256	262
$[NiL_2](NCS)_2$	288	212	186
$NiL(NCS)_2$	307	258	248

species (Fig. 6) as intermediate. These mono-triamine species, collected by the temperature arrest technique in the solid state, yield $Ni(dpt)AO_4 \cdot 3H_2O$ (A is S or Se) on storage in open atmosphere. Both the mono species are identical to their corresponding mono-analogues prepared from aqueous solution.

The thermal stability of $[Ni(dpt)_2]X_2$ (X is Cl, Br, I, NO_3, NCS $0.5SO_4$ or $0.5SeO_4$) with respect to T_i (initial temperature of decomposition) follows the trend $I > Br > NO_3 > SeO_4 > SO_4 > Cl > NCS$ (see Table 4).

$Ni(dpt)X_2 \cdot H_2O$ (X is Br or I), $Ni(dpt)(NO_3)_2 \cdot 2H_2O$ and $Ni(dpt)AO_4 \cdot 3H_2O$ (A is S or Se) become anhydrous upon heating (Table 2). The anhydrous species absorb water molecules readily from the atmosphere. All the dehydrated species on further heating decompose either to their corresponding metal salts or oxides. The decomposition of mono-iodo species shows an exothermic peak followed by endothermic peak as for $Ni(dpt)Cl_2$ (**1b**). This exothermic behaviour shown in the initial stage of decomposition (Fig. 5) does not disappear on hydration. The stability of mono-triamine species follows the order $Br > Cl > NCS > SO_4 > SeO_4 > I > NO_3$.

4. Conclusions

The thermal stabilities of the bis-triamine and also the mono-triamine complexes of Ni(II) decrease as follows: 5,5 (dien) > 5,6 (aepn) > 6,6 (dpt) chelate rings (Table 4) in the same order and as previously found in a solution study. It is also to be noted that a good number of dien complexes undergo phase transition phenomena due to either conformational changes of the chelate rings or geometrical isomerism. The number of complexes which show such transformations is lower with aepn and with dpt there are even fewer, perhaps because of the lower decomposition temperature of the latter two triamine complexes (aepn and dpt), i.e. the complexes decompose before the probable transformation which could have occurred.

Acknowledgement

This project was funded by the C.S.I.R., New Delhi, India.

References

[1] A. Vacca, D. Arenare and P. Paoletti, Inorg. Chem., 5 (1966) 1384.
[2] P. Paoletti, F. Nuzzi and A. Vacca, J. Chem. Soc. A, (1966) 1385.
[3] S. Koner, A. Ghosh and N. Ray Chauduri, Transition Met. Chem., 13 (1988) 291.
[4] S. Koner, A. Ghosh and N. Ray Chaudhuri, Transition Met. Chem., 15 (1990) 394.
[5] A.K. Mukherjee, S. Koner, A. Ghosh, N. Ray Chaudhuri, M. Mukherjee and A.J. Welch, J. Chem. Soc. Dalton Trans., (1994) 2367.
[6] S. Koner, C. Pariya and N. Ray Chaudhuri, Thermochim. Acta, 219 (1993) 261.
[7] C. Pariya, A. Ghosh, S. Ganguli and N. Ray Chaudhuri, Thermochim. Acta, 242 (1994) 195, and references cited therein.
[8] N.F. Curtis, R.W. Hay and Y.M. Curtis, J. Chem. Soc. A, (1968) 182.
[9] S. Biagini and M. Cannas, J. Chem. Soc. A, (1970) 2398.
[10] N.F. Curtis and Y.M. Curtis, Aust. J. Chem., 19 (1966) 1423.
[11] K. Nakamoto, Infrared and Raman Spectra of Inorganic and Coordination Compounds, Wiley-Interscience, New York, 1977, pp. 318, 322.
[12] M. Cannas, G. Marongiu and G. Saba, J. Chem. Soc. Dalton Trans., (1980) 2090.
[13] N.F. Curtis and Y.M. Curtis, Inorg. Chem., 4 (1965) 804.
[14] N.F. Curtis and H.K.J. Powell, J. Chem. Soc. A, (1968) 3070.